

FedCVU: Federated Learning for Cross-View Video Understanding

Shenghan Zhang^{1,*} Run Ling^{1,*} Ke Cao² Ao Ma^{3,†} Zhanjie Zhang^{4,†}

¹Software College, Northeastern University, Shenyang, China

²University of Science and Technology of China, Hefei, China

³University of Chinese Academy of Sciences, Beijing, China

⁴Zhejiang University, Hangzhou, China

zhangsh24@mails.neu.edu.cn, runling001@hotmail.com

Abstract—Federated learning (FL) has emerged as a promising paradigm for privacy-preserving multi-camera video understanding. However, applying FL to cross-view scenarios faces three major challenges: (i) heterogeneous viewpoints and backgrounds lead to highly non-IID client distributions and overfitting to view-specific patterns, (ii) local distribution biases cause misaligned representations that hinder consistent cross-view semantics, and (iii) large video architectures incur prohibitive communication overhead. To address these issues, we propose FedCVU, a federated framework with three components: VS-Norm, which preserves normalization parameters to handle view-specific statistics; CV-Align, a lightweight contrastive regularization module to improve cross-view representation alignment; and SLA, a selective layer aggregation strategy that reduces communication without sacrificing accuracy. Extensive experiments on action understanding and person re-identification tasks under a cross-view protocol demonstrate that FedCVU consistently boosts unseen-view accuracy while maintaining strong seen-view performance, outperforming state-of-the-art FL baselines and showing robustness to domain heterogeneity and communication constraints.

Index Terms—Federated Learning, Cross-View Video Understanding, Selective Layer Aggregation

I. INTRODUCTION

Federated learning (FL) has emerged as a promising paradigm for privacy-preserving collaborative model training without centralizing raw data [1], enabling applications in sensitive domains such as healthcare [2], finance [3], and computer vision [4]. In video understanding, FL is particularly appealing for multi-camera systems where centralizing footage is often infeasible due to privacy regulations or bandwidth constraints [5], [6]. By allowing each camera or site to train locally while sharing only model updates, FL mitigates the risk of data leakage and enables large-scale collaboration across distributed video streams.

However, applying FL to cross-view video understanding faces three major challenges. First, multi-camera video streams exhibit large variations in viewpoint, background, illumination, and scene composition [7], [8]. Such variations are not random but are tightly coupled with camera geometry and deployment environments, resulting in highly structured and persistent feature shifts across clients. This form of heterogeneity leads to highly non-IID client distributions that impede optimization and cause models to overfit to view-specific patterns [9],

[10], thereby limiting generalization to unseen camera views. Second, even with shared model updates, the representations learned by different clients often remain misaligned due to local distribution biases. In cross-view settings, semantically identical actions or identities may exhibit drastically different visual appearances across viewpoints, making it difficult for standard FL aggregation to induce consistent representations. As a result, the global model may converge to view-dependent features that fail to capture cross-view semantics [11], [12]. Third, modern video architectures such as 3D convolutional networks [13] and vision transformers [14], [15] contain tens to hundreds of millions of parameters. Directly synchronizing such large models across many clients incurs prohibitive communication overhead in each FL round [16], which is further exacerbated by the slow convergence typically observed under severe non-IID conditions. These challenges are closely intertwined, posing obstacles to deploying FL-based solutions for real-world multi-camera video understanding systems.

To address these challenges, we propose FedCVU, a federated framework for cross-view video understanding. FedCVU integrates three key components. *View-Specific Normalization (VS-Norm)* preserves client-specific normalization parameters while aggregating the rest, reducing view-dependent distribution gaps and enhancing generalization to unseen cameras. *Cross-View Contrastive Alignment (CV-Align)* introduces a lightweight contrastive loss that encourages consistent representations across clients, mitigating semantic misalignment. *Selective Layer Aggregation (SLA)* dynamically selects layers for aggregation under a communication budget, substantially lowering overhead while maintaining accuracy. Together, these modules jointly address domain heterogeneity, representation inconsistency, and communication efficiency, providing a principled solution for multi-camera video understanding.

We evaluate FedCVU under a cross-view protocol on two representative tasks: action understanding and person re-identification. Across both datasets, FedCVU achieves consistent gains on unseen-view accuracy while preserving strong performance on seen views. Compared with competitive federated baselines, it further attains higher accuracy with substantially reduced communication cost, confirming its robustness to domain heterogeneity, representation misalignment, and

bandwidth constraints. Our main contributions are summarized as follows:

- We introduce FedCVU, a federated framework for cross-view video understanding that addresses the key challenges of domain heterogeneity, representation misalignment, and communication overhead.
- We develop three dedicated modules: VS-Norm for mitigating view-specific distribution gaps, CV-Align for enforcing cross-view representation alignment, and SLA for reducing communication cost through selective aggregation.
- We conduct comprehensive experiments on action understanding and person re-identification tasks under a cross-view evaluation protocol, demonstrating consistent gains in unseen-view accuracy with competitive seen-view performance over strong FL baselines.

II. RELATED WORKS

A. Federated Learning

Federated Learning (FL) enables collaborative training without sharing raw data [1], but suffers from performance degradation under non-IID data. Prior work improves robustness through optimization strategies such as proximal regularization [9], variance reduction [10], dynamic regularization [17], and adaptive server updates [18]. These methods mainly stabilize training across heterogeneous clients, yet overlook structured feature shifts caused by different acquisition conditions. Personalization methods further address heterogeneity. FedBN [19] retains local normalization statistics, while MOON [20] introduces contrastive objectives for representation consistency. However, most approaches are designed for image tasks and do not explicitly model cross-view semantic alignment in federated video settings. Our work focuses on view-induced heterogeneity and representation misalignment in federated video understanding.

B. Cross-View Video Understanding

Cross-view video understanding has been widely studied in centralized settings, especially for action recognition and person re-identification. Existing methods learn view-invariant representations via metric learning or feature alignment [7], [8], [12], supported by benchmarks such as MCAD [21] and MARS [22]. These approaches rely on centralized multi-view data and joint optimization across cameras, which is incompatible with federated settings where data are isolated. Consequently, independently trained client models may produce misaligned representations after aggregation. Our method explicitly models cross-view consistency under federated constraints to improve generalization to unseen views.

III. METHOD

A. Problem Formulation

We study cross-view federated video understanding, where C clients collaboratively train a global video classification model without sharing raw footage. Client c holds a local dataset $\mathcal{D}^c = \{(x_j^c, y_j^c)\}_{j=1}^{n_c}$, where $x_j^c \in \mathbb{R}^{3 \times T \times H \times W}$ is

a video clip and $y_j^c \in \{1, \dots, K\}$ the class label. Due to differences in viewpoint, background, and illumination, the local data distribution $P_c(x, y)$ varies significantly across clients, leading to a highly non-IID setting that is challenging for standard FL algorithms. Formally, the global optimization objective is:

$$\min_{\theta} \sum_{c=1}^C \frac{n_c}{N} \mathcal{L}_c(\theta), \quad N = \sum_{c=1}^C n_c, \quad (1)$$

where the local classification loss is

$$\mathcal{L}_c(\theta) = \mathbb{E}_{(x,y) \sim \mathcal{D}^c} [-\log p_{\theta}(y|x)]. \quad (2)$$

We adopt a cross-view evaluation protocol in which training is conducted on videos from a subset of viewpoints (*seen views*) and testing on held-out viewpoints (*unseen views*). The main objective is to maximize unseen-view accuracy while maintaining competitive seen-view performance.

B. Federated Framework: FedCVU

We propose FedCVU, a unified federated framework that jointly considers view heterogeneity, representation consistency, and communication efficiency. Instead of handling these factors independently, FedCVU integrates three complementary components that interact within a single training loop. View-Specific Normalization stabilizes local feature statistics across camera views, Cross-View Contrastive Alignment promotes semantic consistency among client representations, and Selective Layer Aggregation prioritizes communication on transferable model components. Together, these designs enable effective cross-view generalization under federated constraints.

1) *View-Specific Normalization*: A key source of heterogeneity in cross-view federated learning arises from distribution shifts in feature statistics across camera viewpoints. Differences in camera placement, illumination conditions, and scene composition induce systematic variations in feature activations, which are directly reflected in normalization statistics. Under standard federated aggregation, averaging all parameters, including normalization layers, forces clients to share global statistics that often misrepresent their local distributions. This mismatch can distort feature scaling and bias intermediate representations toward dominant views, ultimately harming cross-view generalization.

To address this issue, we propose View-Specific Normalization (VS-Norm), which preserves client-specific normalization parameters while aggregating the rest of the model. By decoupling normalization from global synchronization, VS-Norm enables each client to maintain feature statistics that are well aligned with its local camera view, while still participating in collaborative representation learning.

Formally, let $\theta = \{\theta_{\text{norm}}, \theta_{\text{rest}}\}$ denote the global parameters, where θ_{norm} includes the normalization-specific weights. For CNN-based backbones with *Batch Normalization (BN)*, we have $\theta_{\text{BN}} = \{\gamma, \beta, \mu, \sigma\}$ representing scale, shift, and running statistics. In FedCVU, only θ_{rest} is aggregated, while each client c maintains its own normalization parameters θ_{BN}^c :

$$\text{BN}^c(x) = \gamma^c \cdot \frac{x - \mu^c}{\sqrt{(\sigma^c)^2 + \epsilon}} + \beta^c, \quad (3)$$

where μ^c and σ^c are estimated from client c 's local data.

For Transformer-based backbones with *Layer Normalization* (LN), $\theta_{\text{LN}} = \{\gamma, \beta\}$ denotes the affine scale and shift, and each client retains its own copy θ_{LN}^c . This design generalizes VS-Norm across different video architectures without introducing additional parameters or communication cost. By preserving view-specific normalization while sharing higher-level representations, VS-Norm reduces harmful statistical interference across clients and provides a stable foundation for subsequent cross-view representation alignment.

2) *Cross-View Contrastive Alignment*: Even with shared updates, client models often learn misaligned representations due to local distribution biases, making cross-view semantics inconsistent. In cross-view scenarios, samples belonging to the same semantic class may exhibit large appearance variations across camera views, which can cause the global model to drift toward view-dependent features. To alleviate this issue, we introduce Cross-View Contrastive Alignment (CV-Align), a lightweight contrastive regularization scheme that encourages semantic consistency across clients while preserving local training autonomy.

Concretely, given a mini-batch $\{(x_i, y_i)\}$ on client c , we extract representations $h_i = f_\theta(x_i) \in \mathbb{R}^d$. Each class y is associated with a global prototype $z_y \in \mathbb{R}^d$, which summarizes the mean embedding of class y aggregated across clients and communication rounds. These prototypes serve as a shared semantic anchor, enabling indirect alignment among clients without requiring direct data sharing.

During training, prototypes are maintained on the server and updated via exponential moving average (EMA):

$$z_y \leftarrow \mu z_y + (1 - \mu) \cdot \frac{1}{|\mathcal{B}_y|} \sum_{i:y_i=y} h_i, \quad (4)$$

where \mathcal{B}_y denotes the set of samples with label y in the current round, and $\mu \in [0, 1)$ controls the update momentum. This update scheme allows prototypes to evolve smoothly over rounds, providing a stable yet adaptive reference for cross-view alignment.

The alignment loss is defined as a contrastive objective between each local embedding h_i and the prototype set $\{z_y\}$:

$$\mathcal{L}_{\text{CV-Align}} = - \sum_i \log \frac{\exp(\text{sim}(h_i, z_{y_i})/\tau)}{\sum_{y'=1}^K \exp(\text{sim}(h_i, z_{y'})/\tau)}, \quad (5)$$

where $\text{sim}(\cdot, \cdot)$ denotes cosine similarity and τ is a temperature parameter. By pulling embeddings toward their corresponding class prototypes while pushing them away from others, CV-Align promotes view-invariant semantic representations across clients.

Finally, the client's training objective is formulated as

$$\mathcal{L}_c = \mathcal{L}_{\text{CE}} + \mathcal{L}_{\text{CV-Align}}, \quad (6)$$

where \mathcal{L}_{CE} is the standard cross-entropy loss. In this way, CV-Align acts as an auxiliary regularizer that complements the primary classification objective without introducing additional model parameters or communication overhead.

3) *Selective Layer Aggregation*: To alleviate the prohibitive communication cost of large video models, we propose Se-

Algorithm 1: Federated Learning with FedCVU

Input: Clients $\{1, \dots, C\}$ with data $\{\mathcal{D}^c\}$; rounds T ; local epochs E ; SLA budget B ; decision interval τ .

Output: Global model θ and prototypes $\{z_y\}$.

```

1 for round  $t = 1$  to  $T$  do
  // Server  $\rightarrow$  Clients
2 Broadcast global model  $\theta^{(t)}$  and prototypes  $\{z_y\}$ ;
  // Clients (in parallel)
3 for each client  $c$  do
4   VS-Norm: keep local norm parameters frozen
    (others trainable);
5   Local training: for  $E$  epochs, minimize  $(\mathcal{L}_{\text{CE}}$ 
    +  $\mathcal{L}_{\text{CV-Align}}$ ) using  $\{z_y\}$ ;
6   Layer signatures: for each block  $\ell$ , compute
    and keep normalized gradient direction  $\hat{g}_\ell^{c,(t)}$ 
    and norm  $r_\ell^{c,(t)}$ ;
7   Upload updated model  $\theta^{c,(t)}$  (with local norm
    kept local), and signatures  $\{\hat{g}_\ell^{c,(t)}, r_\ell^{c,(t)}\}_\ell$  to
    server;
  // Server: SLA statistics &
  selection
8 Aggregate client signatures to obtain per-block
  agreement  $\kappa_\ell^{(t)}$  and salience  $s_\ell^{(t)}$ ;
9 Compute per-block utility  $u_\ell^{(t)}$  and cost  $b_\ell$ ; if
   $t \bmod \tau = 0$ , select subset  $\mathcal{S}_t$  under budget  $B$  via
  greedy on  $u_\ell^{(t)}/b_\ell$  (always include blocks 1,2 and
  L-1,L);
  // Server: soft weights &
  thresholded gating
10 For each block  $\ell$ , set soft weight  $w_\ell^{(t)}$ :  $w_\ell^{(t)}=1$  if
   $\ell \in \mathcal{S}_t$ ; otherwise use a small weak-sync weight in
   $(0, \lambda]$ ;
11 If  $w_\ell^{(t)} < \eta$ , gate it out this round (no parameter
  upload/download for  $\ell$ ; signatures only), and set
   $\tilde{w}_\ell^{(t)}=0$ ; else  $\tilde{w}_\ell^{(t)}=w_\ell^{(t)}$ ;
  // Server: weighted aggregation
12 Update global blocks:
   $\theta_\ell^{(t+1)} \leftarrow (1 - \tilde{w}_\ell^{(t)})\theta_\ell^{(t)} + \tilde{w}_\ell^{(t)} \cdot \sum_c \frac{n_c}{N} \theta_\ell^{c,(t)}$  for  $\ell$ ;
  // Server: prototype maintenance
13 Update prototypes  $\{z_y\}$  via EMA using client
  embeddings/statistics from round  $t$ ;

```

lective Layer Aggregation (SLA), which selectively synchronizes only the most informative and transferable layers across clients. In cross-view settings, different layers exhibit varying degrees of view sensitivity: shallow and deep layers tend to encode more transferable low-level cues and high-level semantics, while intermediate layers are often strongly affected by viewpoint-specific patterns. Uniform synchronization therefore leads to unnecessary communication and may even harm personalization.

TABLE I

RESULTS ON MCAD (ACTION UNDERSTANDING) AND MARS (PERSON RE-IDENTIFICATION) UNDER THE CROSS-VIEW PROTOCOL WITH 20 CLIENTS. MEAN \pm STD OVER THREE RUNS IS REPORTED. **BOLD** AND UNDERLINE MARK BEST AND SECOND-BEST MEAN VALUES; SCORES WITHIN ONE STD ARE REGARDED AS COMPARABLE. COMM. (GB) IS THE PER-CLIENT COMMUNICATION COST (BF16, UPLOAD+DOWNLOAD) UNTIL CONVERGENCE; R^* IS THE AVERAGE NUMBER OF ROUNDS TO CONVERGE.

| Metric | Oracle | FedAvg | FedProx | SCAFF. | MOON | FedBN | FedDyn | FedOpt | FedCVU |
|--|-------------|----------------|----------------|----------------|----------------|--------------------------------|--------------------------------|----------------|--------------------------------|
| <i>MCAD (Action Understanding)</i> | | | | | | | | | |
| Top-1 (%) | 84.2 | 58.9 \pm 0.3 | 58.6 \pm 0.4 | 80.4 \pm 0.5 | 80.1 \pm 0.4 | <u>81.3\pm0.3</u> | 81.0 \pm 0.5 | 80.8 \pm 0.4 | 83.1\pm0.2 |
| Top-5 (%) | 96.5 | 60.8 \pm 0.1 | 61.2 \pm 0.2 | 91.6 \pm 0.3 | 91.4 \pm 0.2 | <u>92.1\pm0.2</u> | 91.9 \pm 0.2 | 91.7 \pm 0.2 | 94.3\pm0.2 |
| Comm. (GB) | – | 9.7 \pm 0.5 | 9.4 \pm 0.4 | 8.8 \pm 0.4 | 8.6 \pm 0.3 | <u>8.5\pm0.3</u> | 8.3 \pm 0.2 | 8.2 \pm 0.2 | 5.8 \pm 0.1 |
| R^* (rounds) | – | 95 \pm 4 | 97 \pm 4 | 110 \pm 5 | 112 \pm 4 | 118 \pm 4 | 116 \pm 3 | 120 \pm 3 | 112 \pm 3 |
| <i>MARS (Person Re-Identification)</i> | | | | | | | | | |
| mAP (%) | 77.4 | 48.1 \pm 0.5 | 47.9 \pm 0.4 | 69.3 \pm 0.3 | 69.8 \pm 0.3 | 70.5 \pm 0.4 | <u>70.7\pm0.3</u> | 70.2 \pm 0.4 | 73.2\pm0.3 |
| CMC@1 (%) | 89.7 | 63.0 \pm 0.4 | 63.7 \pm 0.3 | 84.1 \pm 0.3 | 84.8 \pm 0.2 | 85.1 \pm 0.3 | <u>85.3\pm0.3</u> | 85.0 \pm 0.2 | 87.4\pm0.2 |
| Comm. (GB) | – | 10.2 \pm 0.5 | 9.9 \pm 0.4 | 9.3 \pm 0.4 | 9.1 \pm 0.3 | 9.0 \pm 0.3 | <u>8.8\pm0.2</u> | 8.6 \pm 0.2 | 6.0 \pm 0.1 |
| R^* (rounds) | – | 102 \pm 4 | 104 \pm 4 | 118 \pm 5 | 120 \pm 4 | 126 \pm 4 | 124 \pm 3 | 129 \pm 3 | 123 \pm 3 |

Instead of transmitting full gradients, each client c extracts *lightweight layer signatures* for block ℓ at round t :

$$\hat{g}_\ell^{c,(t)} = \frac{g_\ell^{c,(t)}}{\|g_\ell^{c,(t)}\|_2}, \quad (7)$$

$$r_\ell^{c,(t)} = \|g_\ell^{c,(t)}\|_2, \quad (8)$$

where $g_\ell^{c,(t)}$ is the local gradient (or parameter update). These signatures capture both the update direction and its magnitude with negligible communication overhead.

On the server, signatures from all clients are aggregated to compute two per-block statistics:

$$\kappa_\ell^{(t)} = \frac{2}{C(C-1)} \sum_{c < c'} \langle \hat{g}_\ell^{c,(t)}, \hat{g}_\ell^{c',(t)} \rangle, \quad (9)$$

$$s_\ell^{(t)} = \left\| \frac{1}{C} \sum_{c=1}^C r_\ell^{c,(t)} \hat{g}_\ell^{c,(t)} \right\|_2, \quad (10)$$

where $\kappa_\ell^{(t)}$ measures cross-client directional agreement, reflecting representation consistency, and $s_\ell^{(t)}$ measures the salience of the aggregated update, reflecting its potential impact on global learning.

We define the utility $u_\ell^{(t)} = \max\{0, \kappa_\ell^{(t)}\} \cdot s_\ell^{(t)}$ and the cost b_ℓ as the bytes of block ℓ . Given a per-round budget B , SLA selects a subset \mathcal{S}_t via a knapsack objective (greedy on $u_\ell^{(t)}/b_\ell$):

$$\mathcal{S}_t = \arg \max_{\mathcal{S}} \sum_{\ell \in \mathcal{S}} u_\ell^{(t)} \quad \text{s.t.} \quad \sum_{\ell \in \mathcal{S}} b_\ell \leq B. \quad (11)$$

To stabilize training, the shallowest (1, 2) and deepest (L-1, L) blocks are always synchronized, and the selection is re-computed every τ rounds.

We adopt two modes of block aggregation: **Strong Synchronization** ($\ell \in \mathcal{S}_t$) with fixed weight 1, and **Weak Synchronization** ($\ell \notin \mathcal{S}_t$) with a capped soft weight:

$$w_\ell^{(t)} = \begin{cases} 1, & \ell \in \mathcal{S}_t, \\ \lambda \sigma(\alpha(\kappa_\ell^{(t)} - \tau_\kappa)), & \ell \notin \mathcal{S}_t, \end{cases} \quad (12)$$

where σ is the sigmoid, τ_κ the agreement threshold, and $\lambda \leq 0.3$ limits weak synchronization.

Thresholded gating: if $w_\ell^{(t)} < \eta$, we drop parameter upload/download for block ℓ in round t (signatures only), and set the effective weight $\tilde{w}_\ell^{(t)}=0$; otherwise $\tilde{w}_\ell^{(t)}=w_\ell^{(t)}$. The global update is

$$\theta_\ell^{(t+1)} = (1 - \tilde{w}_\ell^{(t)}) \theta_\ell^{(t)} + \tilde{w}_\ell^{(t)} \sum_c \frac{n_c}{N} \theta_\ell^{c,(t)}. \quad (13)$$

Overall, SLA prioritizes blocks that are both consistent across clients and cost-effective to communicate, while allowing view-sensitive layers to remain personalized, achieving an effective balance between communication efficiency and cross-view generalization.

Overall Algorithm. The complete training procedure of FedCVU is summarized in Algorithm 1. It follows the standard federated loop of local training and server aggregation, while integrating VS-Norm, CV-Align, and SLA within a unified optimization process. Specifically, VS-Norm stabilizes local feature statistics during client-side training, CV-Align enforces cross-view semantic consistency through prototype-based regularization, and SLA adaptively controls parameter synchronization under a communication budget. Together, these components enable efficient and robust federated learning for cross-view video understanding.

IV. EXPERIMENTS

A. Experimental Setup

Datasets. We evaluate FedCVU on two benchmarks: MCAD [21] for action understanding and MARS [22] for video person re-identification. MCAD contains multi-view surveillance videos, while MARS consists of pedestrian tracklets from 6 cameras. We follow a cross-view protocol, training on *seen* cameras and testing on *unseen* ones. To simulate federated clients, each dataset is split into 20 clients by evenly dividing cameras. Unlike prior works that employ synthetic

Dirichlet splits, we adopt this camera-based partition to better reflect real-world deployment.

Baselines. We compare with *FedAvg* [1], *FedProx* [9], *SCAFFOLD* [10], *MOON* [20], *FedBN* [19], *FedDyn* [17], and *FedOpt* [18], covering proximal regularization, variance reduction, contrastive learning, BN personalization, dynamic regularization, and adaptive server optimization.

Implementation Details. A pretrained 3D VAE encoder extracts frozen video latents. The federated model is a Transformer ($d=512$, $L=12$, $f=4$, ~ 37.8 M params) with a lightweight classification head. Only Transformer and head parameters are aggregated; VS-Norm stats remain local. We train with AdamW (lr=1e-4, weight decay=0.05, cosine decay, 5 local epochs) and use BF16 precision for communication. Metrics are Top-1/Top-5 (MCAD) and mAP/CMC@1 (MARS). Experiments run on $8 \times A100$ GPUs, and results are averaged over three seeds.

B. Overall Performance Comparison

Table I reports the performance of FedCVU and competing methods on MCAD and MARS under the cross-view protocol with 20 clients. FedCVU consistently achieves the best unseen-view performance on both tasks, reaching 83.1% Top-1 accuracy on MCAD and 73.2% mAP on MARS. Compared with strong baselines such as FedBN and FedOpt, FedCVU improves Top-1 accuracy by 1.8–2.3% on MCAD and mAP by 2.5–3.0% on MARS, indicating more effective cross-view generalization. Simple aggregation-based methods such as FedAvg and FedProx converge in fewer communication rounds, but their performance saturates at substantially lower accuracy. This gap highlights their limited ability to cope with severe view-induced non-IID distributions. Methods designed to stabilize federated optimization or improve representation consistency, including SCAFFOLD, MOON, FedBN, FedDyn, and FedOpt, achieve markedly higher accuracy, yet still fall short of FedCVU, especially on unseen views. These results suggest that addressing optimization or normalization alone is insufficient for robust cross-view video understanding.

In terms of efficiency, FedCVU also demonstrates a clear advantage. Despite achieving the highest accuracy, it reduces per-client communication cost to 5.8 GB on MCAD and 6.0 GB on MARS, corresponding to nearly a 40–45% reduction compared with standard FL baselines. Moreover, FedCVU converges within 112–123 rounds, which is comparable to or faster than most strong baselines. As shown in Fig. 1, FedCVU exhibits smooth and stable convergence behavior, achieving a favorable balance between accuracy, robustness, and communication efficiency.

C. Ablation Studies

We analyze the contribution of each module in FedCVU on MCAD and MARS, as shown in Tables II and III. Overall, removing any component leads to consistent performance degradation, indicating that the three modules are complementary rather than redundant.

TABLE II
ABLATION STUDY OF FEDCVU ON MCAD (ACTION UNDERSTANDING).
MEAN \pm STD OVER THREE RUNS.

| Variant | Top-1 (%) | Top-5 (%) | Comm. (GB) |
|----------------------|--------------------------------|--------------------------------|-------------------------------|
| w/o VS-Norm | 81.5 \pm 0.3 | 93.2 \pm 0.3 | 5.9 \pm 0.2 |
| w/o CV-Align | 82.3 \pm 0.3 | 93.6 \pm 0.3 | 5.7 \pm 0.1 |
| w/o SLA | 82.9 \pm 0.2 | 94.0 \pm 0.2 | 8.8 \pm 0.3 |
| FedCVU (Full) | 83.1\pm0.2 | 94.3\pm0.2 | 5.8\pm0.1 |

TABLE III
ABLATION STUDY OF FEDCVU ON MARS (PERSON RE-IDENTIFICATION).
MEAN \pm STD OVER THREE RUNS.

| Variant | mAP (%) | CMC@1 (%) | Comm. (GB) |
|----------------------|--------------------------------|--------------------------------|-------------------------------|
| w/o VS-Norm | 71.8 \pm 0.3 | 86.1 \pm 0.3 | 6.1 \pm 0.1 |
| w/o CV-Align | 71.6 \pm 0.3 | 86.0 \pm 0.3 | 6.0 \pm 0.1 |
| w/o SLA | 72.9 \pm 0.3 | 87.1 \pm 0.2 | 9.3 \pm 0.3 |
| FedCVU (Full) | 73.2\pm0.3 | 87.4\pm0.2 | 6.0\pm0.1 |

On MCAD, removing VS-Norm results in a clear drop of Top-1 accuracy (-1.6%) and Top-5 accuracy (-1.1%), highlighting its effectiveness in mitigating view-specific distribution gaps induced by different camera viewpoints. Eliminating CV-Align also degrades performance (Top-1 -0.8% , Top-5 -0.7%), suggesting that representation alignment further improves cross-view generalization beyond statistical normalization alone. These results indicate that both local feature stabilization and cross-client semantic alignment are important for action understanding under cross-view federated settings.

On MARS, the impact of removing VS-Norm or CV-Align is even more pronounced. Discarding either module leads to a decrease of 1.4–1.6% in mAP and around 0.3% in CMC@1, reflecting the sensitivity of person re-identification to view-dependent appearance variations. This observation confirms that maintaining consistent identity representations across camera views benefits from the combined effects of view-specific normalization and prototype-based alignment.

In contrast, removing SLA yields only marginal accuracy degradation on both datasets (less than 0.3%), while substantially increasing communication cost by more than 50%. This demonstrates that SLA primarily improves communication efficiency without compromising predictive performance. Together, these ablation results show that VS-Norm and CV-Align play a critical role in improving accuracy and robustness, whereas SLA effectively reduces communication overhead, enabling FedCVU to achieve a favorable balance between performance and efficiency.

D. Analysis of Synchronization Frequency

Fig. 2 reports the proportion of rounds in which each block is strongly synchronized under SLA. On MCAD, the curve follows a U-shape: shallow blocks (3–4) and deep blocks (9–10) are frequently synchronized, while mid-level blocks (5–7) are less often selected. This pattern is consistent with the

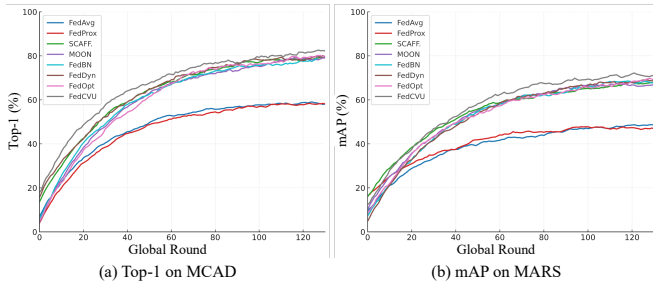


Fig. 1. Convergence curves on MCAD (Top-1) and MARS (mAP). FedCVU converges smoothly within 112–123 rounds and achieves the highest accuracy, while FedAvg/FedProx plateau early at low performance.

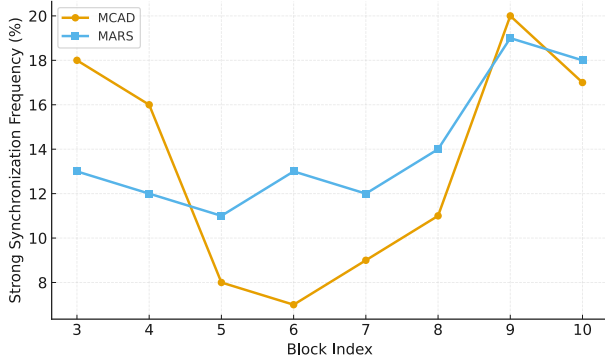


Fig. 2. Strong synchronization frequency across Transformer blocks on MCAD and MARS. MCAD exhibits a U-shaped pattern where shallow and deep blocks are more frequently synchronized, while mid-level blocks remain mostly localized due to higher view-specific variability. In contrast, MARS shows consistently higher synchronization in deeper blocks, reflecting the stability of identity semantics across cameras.

nature of cross-view action understanding, where low-level motion cues and high-level semantics are more transferable across views, whereas mid-level features are highly view-dependent and thus better preserved locally. In contrast, MARS shows a steadily increasing trend toward deeper blocks, with Blocks 9–10 dominating synchronization. This reflects the fact that person re-identification primarily relies on identity-level representations, which are more consistent across clients and therefore favored by SLA. Together, these results confirm that SLA adaptively concentrates communication on the most globally consistent layers while allowing view-specific layers to remain personalized.

V. CONCLUSION

We presented FedCVU, a federated framework for cross-view video understanding that jointly addresses view-induced heterogeneity, representation misalignment, and communication efficiency. FedCVU integrates view-specific normalization, cross-view contrastive alignment, and selective layer aggregation within a unified training process.

REFERENCES

[1] B. McMahan, E. Moore, D. Ramage, S. Hampson, and B. A. y Arcas, “Communication-efficient learning of deep networks from decentralized

data,” in *Artificial intelligence and statistics*. PMLR, 2017, pp. 1273–1282.

[2] N. Rieke, J. Hancox, W. Li, F. Milletari, H. R. Roth, S. Albarqouni, S. Bakas, M. N. Galtier, B. A. Landman, K. Maier-Hein *et al.*, “The future of digital health with federated learning,” *NPJ digital medicine*, vol. 3, no. 1, p. 119, 2020.

[3] Q. Yang, Y. Liu, T. Chen, and Y. Tong, “Federated machine learning: Concept and applications,” *ACM Transactions on Intelligent Systems and Technology (TIST)*, vol. 10, no. 2, pp. 1–19, 2019.

[4] H.-Y. Chen and W.-L. Chao, “On bridging generic and personalized federated learning for image classification,” *arXiv preprint arXiv:2107.00778*, 2021.

[5] Y. Yang, “Privacy-preserving multi-camera vehicle detection for smart cities using federated yolov5s with ua-detrac,” in *2025 3rd International Conference on Image, Algorithms, and Artificial Intelligence (ICIAAI 2025)*. Atlantis Press, 2025, pp. 1149–1156.

[6] N. A. Tu, A. Abu, N. Aikyn, N. Makhanov, M.-H. Lee, K. Le-Huy, and K.-S. Wong, “Fedfslar: A federated learning framework for few-shot action recognition,” in *Proceedings of the IEEE/CVF Winter Conference on Applications of Computer Vision*, 2024, pp. 270–279.

[7] H. Rahmani, A. Mian, and M. Shah, “Learning a deep model for human action recognition from novel viewpoints,” *IEEE transactions on pattern analysis and machine intelligence*, vol. 40, no. 3, pp. 667–681, 2017.

[8] J. Liu, N. Akhtar, and A. Mian, “Viewpoint invariant action recognition using rgb-d videos,” *IEEE Access*, vol. 6, pp. 70 061–70 071, 2018.

[9] T. Li, A. K. Sahu, M. Zaheer, M. Sanjabi, A. Talwalkar, and V. Smith, “Federated optimization in heterogeneous networks,” *Proceedings of Machine learning and systems*, vol. 2, pp. 429–450, 2020.

[10] S. P. Karimireddy, S. Kale, M. Mohri, S. Reddi, S. Stich, and A. T. Suresh, “Scaffold: Stochastic controlled averaging for federated learning,” in *International conference on machine learning*. PMLR, 2020, pp. 5132–5143.

[11] J. Li, Y. Wong, Q. Zhao, and M. S. Kankanhalli, “Unsupervised learning of view-invariant action representations,” *Advances in neural information processing systems*, vol. 31, 2018.

[12] L. Wu, R. Hong, Y. Wang, and M. Wang, “Cross-entropy adversarial view adaptation for person re-identification,” *IEEE Transactions on Circuits and Systems for Video Technology*, vol. 30, no. 7, pp. 2081–2092, 2019.

[13] D. Tran, L. Bourdev, R. Fergus, L. Torresani, and M. Paluri, “Learning spatiotemporal features with 3d convolutional networks,” in *Proceedings of the IEEE international conference on computer vision*, 2015, pp. 4489–4497.

[14] A. Dosovitskiy, L. Beyer, A. Kolesnikov, D. Weissenborn, X. Zhai, T. Unterthiner, M. Dehghani, M. Minderer, G. Heigold, S. Gelly *et al.*, “An image is worth 16x16 words: Transformers for image recognition at scale,” *arXiv preprint arXiv:2010.11929*, 2020.

[15] A. Arnab, M. Dehghani, G. Heigold, C. Sun, M. Lučić, and C. Schmid, “Vivit: A video vision transformer,” in *Proceedings of the IEEE/CVF international conference on computer vision*, 2021, pp. 6836–6846.

[16] J. Konečný, H. B. McMahan, F. X. Yu, P. Richtárik, A. T. Suresh, and D. Bacon, “Federated learning: Strategies for improving communication efficiency,” *arXiv preprint arXiv:1610.05492*, 2016.

[17] D. A. E. Acar, Y. Zhao, R. M. Navarro, M. Mattina, P. N. Whatmough, and V. Saligrama, “Federated learning based on dynamic regularization,” *arXiv preprint arXiv:2111.04263*, 2021.

[18] S. Reddi, Z. Charles, M. Zaheer, Z. Garrett, K. Rush, J. Konečný, S. Kumar, and H. B. McMahan, “Adaptive federated optimization,” *arXiv preprint arXiv:2003.00295*, 2020.

[19] X. Li, M. Jiang, X. Zhang, M. Kamp, and Q. Dou, “Fedbn: Federated learning on non-iid features via local batch normalization,” *arXiv preprint arXiv:2102.07623*, 2021.

[20] Q. Li, B. He, and D. Song, “Model-contrastive federated learning,” in *Proceedings of the IEEE/CVF conference on computer vision and pattern recognition*, 2021, pp. 10 713–10 722.

[21] W. Li, Y. Wong, A.-A. Liu, Y. Li, Y.-T. Su, and M. Kankanhalli, “Multi-camera action dataset for cross-camera action recognition benchmarking,” in *2017 IEEE winter conference on applications of computer vision (WACV)*. IEEE, 2017, pp. 187–196.

[22] L. Zheng, Z. Bie, Y. Sun, J. Wang, C. Su, S. Wang, and Q. Tian, “Mars: A video benchmark for large-scale person re-identification,” in *European conference on computer vision*. Springer, 2016, pp. 868–884.

- [23] T. Chen, S. Kornblith, M. Norouzi, and G. Hinton, "A simple framework for contrastive learning of visual representations," 2020. [Online]. Available: <https://arxiv.org/abs/2002.05709>
- [24] K. He, H. Fan, Y. Wu, S. Xie, and R. Girshick, "Momentum contrast for unsupervised visual representation learning," 2020. [Online]. Available: <https://arxiv.org/abs/1911.05722>
- [25] A. Radford, J. W. Kim, C. Hallacy, A. Ramesh, G. Goh, S. Agarwal, G. Sastry, A. Askell, P. Mishkin, J. Clark, G. Krueger, and I. Sutskever, "Learning transferable visual models from natural language supervision," 2021. [Online]. Available: <https://arxiv.org/abs/2103.00020>
- [26] J. Snell, K. Swersky, and R. S. Zemel, "Prototypical networks for few-shot learning," 2017. [Online]. Available: <https://arxiv.org/abs/1703.05175>
- [27] Q. Li, B. He, and D. Song, "Model-contrastive federated learning," 2021. [Online]. Available: <https://arxiv.org/abs/2103.16257>
- [28] J. Ho, A. Jain, and P. Abbeel, "Denoising diffusion probabilistic models," 2020. [Online]. Available: <https://arxiv.org/abs/2006.11239>
- [29] R. Rombach, A. Blattmann, D. Lorenz, P. Esser, and B. Ommer, "High-resolution image synthesis with latent diffusion models," 2022. [Online]. Available: <https://arxiv.org/abs/2112.10752>
- [30] J. Feng, A. Ma, J. Wang, K. Cao, and Z. Zhang, "Fancyvideo: Towards dynamic and consistent video generation via cross-frame textual guidance," 2025. [Online]. Available: <https://arxiv.org/abs/2408.08189>
- [31] R. Ling, K. Cao, J. Lu, A. Ma, H. Liu, R. He, C. Wang, R. Xu, Y. Shao, Z. Zhang, P. Wu, G. Guo, W. Feng, Z. Zhang, J. Lv, J. Shen, C. Law, and X. Wang, "Mofu: Scale-aware modulation and fourier fusion for multi-subject video generation," 2025. [Online]. Available: <https://arxiv.org/abs/2512.22310>
- [32] J. Wang, A. Ma, K. Cao, J. Zheng, Z. Zhang, J. Feng, S. Liu, Y. Ma, B. Cheng, D. Leng, Y. Yin, and X. Liang, "Wisa: World simulator assistant for physics-aware text-to-video generation," 2025. [Online]. Available: <https://arxiv.org/abs/2503.08153>
- [33] Y. Wang, L. Zhang, J. Liu, J. Yan, Z. Zhang, J. Zheng, A. Ma, R. Ling, X. Yang, D. Wu, X. Chen, and X. Li, "Video-em: Event-centric episodic memory for long-form video understanding," 2026. [Online]. Available: <https://arxiv.org/abs/2508.09486>
- [34] J. Wang, A. Ma, J. Feng, D. Leng, Y. Yin, and X. Liang, "Qihoo-t2x: An efficient proxy-tokenized diffusion transformer for text-to-any-task," 2024. [Online]. Available: <https://arxiv.org/abs/2409.04005>
- [35] K. Cao, J. Wang, A. Ma, J. Feng, X. He, R. Ling, H. Liu, J. Lu, W. Feng, H. Wang, H. Pei, Y. Shao, Z. Zhang, and J. Zhang, "Relactrl: Relevance-guided efficient control for diffusion transformers," 2026. [Online]. Available: <https://arxiv.org/abs/2502.14377>
- [36] R. Ling, W. Wang, Y. Liu, G. Guo, H. Liu, J. Lu, Q. Zhang, Y. Xu, S. Lu, Y. Wang, Y. Shao, Z. Zhang, A. Ma, L. Jiang, and X. Wang, "Ragar: Retrieval augmented personalized image generation guided by recommendation," 2025. [Online]. Available: <https://arxiv.org/abs/2505.01657>
- [37] Z. Zhang, A. Ma, K. Cao, J. Wang, S. Liu, Y. Ma, B. Cheng, D. Leng, and Y. Yin, "U-stydit: Ultra-high quality artistic style transfer using diffusion transformers," 2025. [Online]. Available: <https://arxiv.org/abs/2503.08157>

A. Relation to Contrastive Representation Learning

Recent advances in contrastive learning, including SimCLR [23], MoCo [24], and CLIP [25], have demonstrated the effectiveness of learning transferable representations by maximizing agreement between semantically related samples while separating unrelated ones. These methods typically rely on large-scale centralized data and instance-level or cross-modal alignment, enabling strong generalization across domains and tasks.

Beyond instance-level contrastive objectives, extensions to supervised and prototype-based settings [26] further improve semantic consistency by explicitly leveraging class-level structure. Such approaches replace pairwise matching with alignment to class centers or prototypes, providing a more stable and semantically meaningful learning signal, especially under intra-class variation.

In federated learning, contrastive methods such as MOON [27] have been introduced to alleviate client drift by enforcing consistency between local and global representations. However, existing approaches mainly focus on model-level alignment and do not explicitly address structured feature shifts caused by heterogeneous data distributions, such as those induced by different camera views in video scenarios.

Our CV-Align builds upon these lines of work by introducing a prototype-based contrastive mechanism tailored for cross-view federated settings. Instead of relying on shared data or direct sample matching, CV-Align maintains global class prototypes as lightweight semantic anchors, enabling consistent alignment across clients with disjoint and heterogeneous data. This design bridges supervised contrastive learning and federated optimization, and is particularly suited for cross-view video understanding where semantically identical patterns may exhibit substantial appearance variation across viewpoints.

B. Relation to Video and Image Generation Models

Recent progress in image and video generation has been largely driven by diffusion models and diffusion transformers, which enable high-fidelity synthesis through iterative denoising and powerful latent representations [28], [29]. These models have been extended to video generation, where additional challenges such as temporal consistency, multi-subject interaction, and long-range coherence arise.

To address these challenges, a number of recent works have explored structured control and representation learning within generative frameworks. For example, methods such as FancyVideo [30] and MoFu [31] improve temporal consistency and multi-subject generation through cross-frame guidance and frequency-aware fusion. WISA [32] introduces physics-aware simulation priors to enhance realism, while VideoEM [33] focuses on long-form video understanding via persistent memory mechanisms. Efficiency-oriented designs, such as Qihoo-T2X [34] and RelaCtrl [35], further improve scalability by reducing redundant computation or introducing relevance-guided control. In the image domain, works like RAGAR [36]

and U-StyDiT [37] explore personalization and high-quality style transfer within diffusion transformer frameworks.

Despite these advances, most existing methods assume centralized training with access to large-scale datasets, and rely on shared representations or explicit conditioning to achieve cross-view or multi-condition consistency. In contrast, real-world multi-camera or multi-source scenarios often involve distributed and privacy-sensitive data, where centralized training is infeasible.

Our FedCVU framework provides a complementary perspective by addressing representation consistency under federated constraints. In particular, the proposed CV-Align introduces prototype-based alignment to enforce cross-view semantic consistency without sharing raw data, while VS-Norm stabilizes view-specific feature distributions. These properties are directly relevant to generative modeling, where maintaining consistent identity, motion, and semantics across views or conditions is critical. Therefore, FedCVU can be viewed as a step toward federated generative modeling, offering a potential pathway to extend diffusion-based video and image generation to distributed settings with heterogeneous data sources.

C. Generalization to Generative and Multi-Modal Settings

Although FedCVU is evaluated on discriminative tasks such as action understanding and person re-identification, its core design is not limited to classification settings. The proposed framework addresses a more general problem: learning consistent and transferable representations under heterogeneous and distributed data distributions.

In generative modeling, especially in video and image generation, maintaining semantic consistency across conditions, views, or modalities is a fundamental challenge. For example, multi-view video generation requires preserving identity and motion coherence across viewpoints, while text-to-video models must align visual content with semantic conditions over time. These requirements are closely related to the cross-view representation alignment problem studied in this work.

The components of FedCVU can be naturally extended to such scenarios. VS-Norm provides a mechanism to handle condition-specific or domain-specific feature shifts, which are common in multi-modal or multi-view generation. CV-Align offers a lightweight way to enforce semantic consistency without requiring shared data, making it suitable for distributed generative training. Meanwhile, SLA enables efficient communication by prioritizing globally consistent and transferable components, which is particularly important for large-scale generative models with high communication cost.

These properties suggest that FedCVU can serve as a general framework for federated representation learning beyond discriminative tasks. In particular, it provides a promising direction for extending diffusion-based generative models and multi-modal learning systems to federated settings, where data are inherently decentralized and heterogeneous.